

JAERI-M

6 6 4 7

THE STUDY OF DISCHARGE CLEANING IN THE JFT-2
TOKAMAK WITH SURFACE OBSERVATION BY AES

July 1976

Y. GOMAY*, T. TAZIMA, N. FUJISAWA,
N. SUZUKI, S. KONOSHIMA

この報告書は、日本原子力研究所が JAERI-M レポートとして、不定期に刊行している研究報告書です。入手、複製などのお問い合わせは、日本原子力研究所技術情報部（茨城県那珂郡東海村）あて、お申しこしてください。

JAERI-M reports, issued irregularly, describe the results of research works carried out in JAERI. Inquiries about the availability of reports and their reproduction should be addressed to Division of Technical Information, Japan Atomic Energy Research Institute, Tokai-mura, Naka-gun, Ibaraki-ken, Japan.

The Study of Discharge Cleaning in the JFT-2 Tokamak
with Surface Observation by AES

Yoshio GOMAY*, Teruhiko TAZIMA, Noboru FUJISAWA⁺,
Norio SUZUKI⁺ and Shigeru KONOSHIMA⁺

Division of Large Tokamak Development, Tokai, JAERI

(Received July 7, 1976)

Noticeable correlations were observed between the changes of discharge characteristics, wall conditions and typical mass peaks with discharge cleaning in the JFT-2 tokamak. Atomic composition of the vacuum wall surface observed by AES becomes constant with continuing discharge cleaning in the level except hydrogen and helium: 30-50 % C, 20-30 % Mo, 15-30 % stainless steel elements and 10-15 % O. The stable reproducible plasma with $Z_{\text{eff}} = 4.5$ was obtained in this wall condition. The limiter and vacuum wall materials (Mo and 304 stainless steel, respectively), carbon and oxygen were observed depositing on the wall in the thickness of about 300 Å at the minimum inner radius of the vacuum chamber and 40 Å nearly at the maximum after 2900 cleaning pulses. The mechanism determining the wall condition is also discussed.

*) On leave from Research and Development Centre, Tokyo Shibaura Electric Co., Ltd.

+ Division of Thermonuclear Fusion Research, Tokai, JAERI.

壁状態のAES観察を含むJFT-2
放電洗浄効果実験

日本原子力研究所東海研究所大型トカマク開発部

五明由夫*・田島輝彦・藤沢 登+
鈴木紀男+・木島 滋+

(1976年7月7日受理)

JFT-2トカマクの放電洗浄過程で、放電特性、壁状態、放電により雰囲気へ放出されるガス成分の変化を観察することにより、放電洗浄の効果を統一的に示した。壁表面の組成は、放電洗浄を続けるにしたがって一定の状態（原子組成；30～50%C，20～30%Mo，15～30%SUS構成元素，10～15%O，但し，H，Heは除く）を保つようになり、その状態で $Z_{\text{eff}} = 4.5$ の安定で再現性のよいプラズマが得られた。放電洗浄中壁位置でプラズマにさらしたサンプルには、ペロー山位置で約 300 \AA ，谷位置で 40 \AA の、リミター材（Mo），壁材（SUS系），炭素，酸素で構成される堆積層が観測された。壁状態の決定機構についても考察した。

*） 外来研究員 東芝総合研究所

+） 日本原子力研究所東海研究所 核融合研究部

目次なし

1. INTRODUCTION

Plasma-wall interaction plays an important role in the present tokamak discharges and will be more important in future large tokamaks with higher plasma temperatures and longer discharge durations. Impurity concentrations in the plasma should depend on the plasma characteristics, especially at the boundary region, and the surface condition of the limiter and vacuum wall. A well conditioned wall surface should therefore be necessary for attaining a stable plasma with low impurity concentrations. Baking of the vacuum chamber and/or discharge cleaning have been employed for the purpose in current tokamak devices. It has been shown in the ATC that an active metal coating evaporated onto the surface of the vacuum chamber is a simple technique to reduce the impurity concentrations in the plasma [1].

In this paper the effect of discharge cleaning in the JFT-2 tokamak is studied by observing the changes with cleaning pulses in the discharge characteristics, the surface compositions of the samples located at the vacuum wall and the typical mass peaks. We also discuss the mechanism determining the condition of the vacuum wall surface in view of the observed depth profiles of atomic compositions in the samples.

The same kind of research was recently initiated in the PULSATOR [2,3] mainly as to the material transport during discharges, and the deposition of the limiter and wall materials and oxygen has been observed on the target exposed to the plasma. The wall problems of the Intersecting Storage Rings (ISR) at CERN have been studied [4]. Some cleaning methods for stainless steel including glow discharge cleaning have been studied by SIMS and AES with a view to providing a clean wall surface with low gas desorption under ion bombardment [5].

2. EXPERIMENTAL DETAILS

The JFT-2 device has been described in detail elsewhere [6] except that the toroidal magnetic field has been increased up to 18 kG. This experiment was performed in baking the vacuum chamber and following discharge cleaning after opening the torus to air for three months (Sep. - Dec., 1975). The base pressure, 5×10^{-8} Torr, was obtained after baking the chamber itself at 150 - 200°C and the observation sections at about 80°C. The pumping speed by a turbomolecular pump with a liquid nitrogen trap is about 1000 l/sec in high vacuum pressure (10^{-4} - 10^{-6} Torr) but is decreased to 100 - 200 l/sec at the base pressure. The

discharge conditions for cleaning are: toroidal magnetic field = 6 - 7 kG, filling pressure = 2×10^{-4} Torr (hydrogen); plasma current = 100 KA; and repetition time = 1 - 1.5 min. The total cleaning pulses are 2900 shots.

The discharge characteristics were measured at the typical stages of discharge cleaning in the same conditions as in cleaning pulses except that the toroidal magnetic field is 14 kG. We observed the electron temperature and density profiles vertically at $\phi = 270^\circ$ (starting clockwise from the limiter) by Thomson scattering; the latter also horizontally at $\phi = 180^\circ$ by a microwave interferometer; and radiation losses at $\phi = 180^\circ$ by a silicon thermister bolometer [19].

The surface compositions of the samples were measured by Auger Electron Spectroscopy (AES) at the outer side of the toroidal field coils ($\phi = 90^\circ$), using the movable mechanism of the samples as shown in Fig. 1a. The Auger electron spectrometer is a standard cylindrical mirror analyzer (Physical Electronics Inc.). The primary electron energy for AES is 4 keV. The samples of 304 stainless steel and molybdenum are located as shown in Fig. 1b, simulating the wall at the minimum and maximum inner radius of the vacuum chamber (304ss bellows). The vacuum pressure in the chamber for AES measurement is $10^{-6} - 10^{-7}$ Torr. The depth profiles of atomic compositions in the samples were also measured after discharge cleaning, using Auger/sputter techniques [7] in the standard system of the method (Physical Electronics Inc.). The argon ion beam was used for sputter-etching in the conditions: Ar pressure = 5×10^{-5} Torr; beam energy = 2 keV; and emission current = 15 or 30 mA. The base pressure of the system is 10^{-9} Torr.

The time dependence of the mass peaks which are identified to be CH_3^+ and CH_4^+ from the mass spectrum, was measured in the intervals of discharges by a quadrupole mass filter located at the evacuation port ($\phi = 0^\circ$).

3. THE EFFECT ON DISCHARGE CHARACTERISTICS

The time behaviours of the loop voltage and total plasma current including the liner one drastically change with cleaning pulses as shown in Fig. 2. The initial resistive plasma becomes inductive within 500 shots as observed in the decrease of loop voltage and the increase of current duration. The time behaviours change gradually thereafter and become constant at about 1500 shots. Figure 3 shows the changes with cleaning pulses in the central electron temperature, the plasma resistance at the peak of plasma current and the radiation losses integrated

temporally during the discharge and spatially on the assumption that the distribution is homogeneous over the wall. The former increases and the latter two correspondingly decrease with cleaning pulses. This suggests that the impurities in the plasma considerably affect the discharge characteristics at the initial stages of discharge cleaning.

The discharge characteristics at the end of discharge cleaning (after 2500 shots) are shown in Fig. 4. Fig. 4a shows the time behaviours of loop voltage, plasma current, mean line-of-sight density and peak electron temperature and Fig. 4b the electron density and temperature profiles at the peak of plasma current, 22 msec after the start. From these results, the energy confinement time τ_E is 3.2 msec on the assumption that the ion temperature is one third of the electron, the poloidal beta for electrons β_{pe} is 0.17 and the effective ionic charge Z_{eff} is 4.5 with the effect of trapped-particles included, assuming that the current distribution is proportional to $T_e(r)^{3/2}$ and Z_{eff} is constant over the plasma column.

4. CONDITIONS OF THE VACUUM WALL

(A) SURFACE COMPOSITION

Quantitative analysis with AES is not fully established yet, but semi-quantitative analysis is possible with the aid of standard spectra of the elements as published in a handbook [8]. In this method the relative atomic content R_i , denoted by atomic percents, of the element i except hydrogen and helium is obtained by [9]:

$$R_i = \frac{P_i}{S_i} / \sum_{i=1}^n \frac{P_i}{S_i} \times 100 \quad (1)$$

where P_i and S_i are the observed Auger peak height and the relative yield of Auger electrons in each main peak, respectively, and n is the number of the observed elements. Here we assume that the Auger peak shape, the escape depth of Auger electrons and the influence of backscattering on the relative yield in each element are the same as in the cases of standard spectra. The accuracy of the method is expected to be within a factor of two [9].

The surface composition except hydrogen and helium in the samples located at the vacuum wall (Fig. 1b) changes with cleaning pulses as shown in Fig. 5. The surfaces are covered by carbon and sodium in the

composition of more than 90 atomic percent (a/o) before discharge cleaning. This initial contaminated layers are removed with continuing discharge cleaning and then the surface composition is saturated in the level of 30-50 a/o C, 20-30 a/o Mo, 15-30 a/o stainless steel elements and 10-15 a/o O after 200-500 shots in the samples located at the minimum inner radius of the vacuum chamber and 500-1000 shots in the one located nearly at the maximum.

Comparing these results with the changes of the discharge characteristics (Fig. 2), we may consider that the drastic changes of the discharge characteristics observed in the initial 200 shots and succeeding 300 shots are mainly caused by conditioning of the wall near the minimum and maximum inner radius of the vacuum chamber, respectively. We have not enough results to discuss the following gradual changes up to 1500 shots, but homogeneous conditioning throughout the torus may be necessary for obtaining the stable discharges without negative voltage spikes.

We had apprehensions of misunderstanding the surface composition by adsorption of the ambient gas species and deposition of carbon under electron bombardment for AES, since it took 1-2 hours to measure the four samples. These effects were examined in the standard AES/sputter system. After the samples of 304 stainless steel and molybdenum were cleaned by sputter-etching, they were exposed to the almost same vacuum, 2×10^{-7} Torr, as at the measurement in JFT-2 and to electron bombardment for AES in the same vacuum. Fig. 6 shows the time dependence of the surface composition in these processes. Exposed to the vacuum, the cleaned surfaces of both samples are covered with carbon by 20 - 30 a/o and oxygen by 5 a/o in less than a minute and have no change thereafter. Exposed to electron bombardment, the molybdenum surface is gradually covered with carbon up to 60 a/o in 30 minutes. The deposition under electron bombardment cannot be found in the other cases such as carbon or oxygen on the stainless steel surface and oxygen on the molybdenum, since there exists no difference between the results of adsorption and deposition.

These results suggest that the adsorption of ambient gas species cannot considerably affect the data of surface composition (Fig. 5), since it will be almost saturated in the interval of cleaning pulses (1-1.5 min). On the contrary, the deposition of carbon on the molybdenum surface under electron bombardment affects the data in such a poor vacuum pressure for AES measurement as used in JFT-2. The radiation time of primary electron beam was therefore shortened in the measurement as far as possible.

(B) DEPTH PROFILES

Quantitative analysis with Auger/sputter techniques is not fully established for mixed layers, since etching speed is difficult to be estimated and preferential sputtering at etching is inevitable [7]. But we perform it for semi-quantitative discussion, estimating the former from the data for each element and neglecting the latter effect.

Figure 7 shows the depth profiles of atomic compositions in the samples (Fig. 1b) except Mo-B observed after discharge cleaning. Though the samples were exposed to air for three days before the measurement, the contaminated layers on the surface mainly composed by oxygen and sodium is only about 10 \AA in thickness. Under them there exist the deposited layers of the typical atomic composition: 40 - 50 at% Mo, 20 - 30 at% C, 10 - 15 at% Fe, 5 - 10 at% O, and 1 - 5 at% Cr and Ni. In deeper regions there seem to exist semi-bulk layers of each metal (Mo or 304 ss) which contains carbon by 10 at% in every samples. In bulk layers of 304 stainless steel carbon content should be the same order as estimated from the chemical composition (0.06 %C) [11].

The etching speed of argon ion beam (2 keV, 15 mA) is $11 \text{ \AA}/\text{min}$ for molybdenum and $17 \text{ \AA}/\text{min}$ for iron [10]. If the thickness of the deposited layers in the stainless steel samples is defined by the depth where molybdenum content is decreased to 10 at%, it is 300 \AA for SS-B located at the minimum inner radius of the vacuum chamber and 40 \AA for SS-B located nearly at the maximum on the assumption that the etching speed of the layer is $15 \text{ \AA}/\text{min}$. The deposited layers in Mo-A are similar to those in SS-A except that the initially adsorbed sodium remains by about 10 at% at the depth corresponding to initial surface and the decrease of iron content in the layers between the deposited and semi-bulk layers is steeper than that of molybdenum in the same layers of SS-A. The detailed data of Mo-B was not obtained, but it was confirmed that the thickness of the deposited layers is the same as in the case of SS-B.

The mechanism in which the deposited layers are produced may be that the atoms of the limiter and wall materials, leaving each place by interaction with the plasmas, arrive at the wall as ions and the gas species of carbon and oxygen are adsorbed by the active surface in the intervals of discharges. The limiter material may enter into the plasmas by either sputtering due to ions or evaporation caused by localized temperature rise and the wall material mainly by sputtering due to charge exchange neutrals. The particles arriving at the wall are considered to be ions from the fact that the thickness of the deposited layers in the

sample SS-A is about ten times as large as in SS-B. This well corresponds to the results in PULSATOR [3].

The sources of carbon and oxygen should exist in the vacuum chamber, since the contents of carbon and oxygen become constant with continuing discharge cleaning in the surface composition (Fig. 5) and they are also constant over the deposited layers (Fig. 7). The sources may be the ambient gas species, considering that gas species including carbon and oxygen seem to be adsorbed by the surface in view of the difference of molybdenum content in the region of 20 Å from the surface. We can estimate this difference by applying that the escape depths of Auger electrons from molybdenum atom are 5 Å and 20 Å for the energy of 221 eV and 2044 eV, respectively [9]. Calculating molybdenum content with these two Auger peaks, it is suggested that the molybdenum content in the region of 20 Å from the surface is a few times as large as in 5 Å, or more carbon and oxygen exist in shallower region from the surface. The adsorption may also be the reason why the carbon or oxygen content in the surface composition (Fig. 5) is larger than those in the deposited layers (Fig. 7).

The adsorbed carbon seems to form carbide by successive recycling between the plasma and the wall, since Auger peak shape of carbide [12] was observed in the measurement of the depth profiles and of the surface composition after more than several hundreds of cleaning pulses.

The total amount of deposited material for 2900 cleaning pulses at the sample SS-A is nearly 6×10^{16} Mo atoms/cm², 3×10^{16} atoms of stainless steel elements/cm², 10^{17} C atoms/cm², and 10^{16} O atoms/cm². If we assume that the molybdenum particles are deposited uniformly in toroidal direction, the total deposited amount per discharge throughout the torus is about 10^{18} atoms. This nearly corresponds to a tenth of total plasma particles.

As for carbon and oxygen, assuming that they are adsorbed with the sticking probability of 0.1 during discharge cleaning (4 days), the necessary partial pressure for deposition is about 10^{-9} Torr for carbon species and 10^{-10} Torr for oxygen species which can be expected from the mass spectrum at the base pressure shown in Fig. 9.

5. OBSERVATION OF MASS PEAKS

The effect of discharge cleaning has been studied by observing the changes of mass peaks with cleaning pulses including their differences

between before and after the discharge [13]. In this experiment we found that CH_4 released from the wall surface by the discharge is almost evacuated, since the mass peaks of $m/e = 15$ and 16 were observed to increase instantaneously by the discharge and then decrease in accordance with the evacuating speed. Such phenomena were not observed in the other mass peaks, $m/e = 18, 28, 32, 44$ and so on. The peak heights generated by the discharge rapidly decrease in initial 500 shots and become constant thereafter as shown in Fig. 8a. This result is similar to the carbon rate change in the surface composition (Fig. 5). We can well understand this similarity, considering that the peak heights should correspond to the sources of CH_4 on the wall surface.

We have another same kind of data shown in Fig. 8b which were obtained in helium discharge cleaning performed before. The result is similar to that of hydrogen discharge cleaning (Fig. 8a) except that more cleaning pulses are necessary for attaining the nearly constant peak heights.

The constancy of the peak heights observed in both cases suggests that the sources of CH_4 exist in the vacuum chamber. This may be correlated with the sources of carbon and oxygen in the deposited layers (Fig. 7). As described before, these sources may be the ambient gas species in which considerable amount of water and acetone exist as identified from the mass spectrum at the base pressure shown in Fig. 9. This may be caused by the low baking temperature ($\sim 80^\circ\text{C}$) of the observation sections.

6. CONCLUSION AND DISCUSSION

It has been shown that there exists noticeable correlation between the changes of discharge characteristics, wall conditions and methane emission by the discharge with discharge cleaning using low toroidal magnetic field. The surface condition of the vacuum wall becomes constant with continuing discharge cleaning and the stable reproducible plasma with $Z_{\text{eff}} = 4.5$ was obtained in this saturated wall condition. The discharge characteristics, especially Z_{eff} , will not be further improved by continuing discharge cleaning.

The limiter and wall materials, carbon and oxygen deposit on the samples exposed to the plasma at the vacuum wall during discharge cleaning. Considering the results throughout this paper, the saturated level of the wall condition may be determined by deposition of the metallic materials

during the discharges and adsorption of the ambient gas species in the intervals of discharges.

In order to obtain a clean wall surface by discharge cleaning, it is necessary to suppress contamination by the ambient gas species. Higher vacuum, higher wall temperature and using more continuous discharges such as radio frequency and glow ones are preferable for suppressing adsorption. Filling gas species for discharges are also important for producing volatile materials on a wall surface.

Considering from the results of this paper, in-situ coating of the first wall by suitable material is another potential method for obtaining a clean wall surface as shown in the ATC [1].

The existence of oxygen and carbon as impurities in the plasmas has been confirmed in JFT-2 [6, 14] and it was recently shown that the main impurity may be oxygen [18] as observed in other tokamak devices [15, 16]. It is still an open problem why more oxygen is desorbed from the wall than carbon in spite of less oxygen on the wall surface. A possible mechanism is chemical effect such as H_2O formation on the wall surface by particle bombardment [17].

It is interesting from another point of view that the strongly adsorbed carbon, supposed from the fact that the Auger peak shape of carbide was observed, may have a small desorption yield with plasma-wall interaction, comparing with the case of adsorbed oxygen. This may suggest that the metal, which strongly adsorbs carbon and has negligible oxygen on the surface, is feasible for the first wall.

ACKNOWLEDGEMENT

We would like to acknowledge many interesting and stimulating discussions with our colleagues. In particular, we would like to thank: T. Matoba, who contributed the data by Thomson scattering; T. Sato, who contributed the data by bolometer; T. Narusawa (ULVAC Co.), who contributed the data by AES; and the JFT-2 operating team led by N. Toyoshima and S. Kunieda.

We are also grateful to Drs. Y. Tuzi (Univ. of Tokyo) and S. Komiya (ULVAC Co.) for their stimulating discussions and Drs. S. Mori and M. Yoshikawa for their continuing encouragement in this work.

REFERENCES

- [1] STOTT, P. E., DAUGHNEY, C. C., ELLIS, Jr. R. A. Nucl. Fusion 15 (1975) 431.
- [2] STAIB, P., BEHRISCH, R., HEILAND, W., STAUDENMAIER, G., Proc. 7th European Conf. on Controlled Fusion and Plasma Physics Lausanne (1975) 133.
- [3] STAIB, PH., STAUDENMAIER, G., Program Summaries of Int. Conf. on Surface Effects in Controlled Thermonuclear Devices, San Francisco (1976) 19.
- [4] CALDER, R. S., Vacuum 24 (1974) 437.
- [5] MATHEWSON, A. G., Vacuum 24 (1974) 505
- [6] FUJISAWA, N., et al., Plasma Phys. and Controlled Nuclear Fusion Research 1974, 5th Conf. Proc. Tokyo, 1, 3.
- [7] HOLLOWAY, D. M., J. Vac. Sci. Technol. 12 (1975) 392.
- [8] PALMBERG, P. W., RIACH, G. E., WEBER, R. E., MACDONALD, N. C., Handbook of Auger Electron Spectroscopy, Physical Electronics Inc. (1972).
- [9] PALMBERG, P. W., Anal. Chem. 45 (1973) 549.
- [10] Technical Data of Physical Electronics Inc.
- [11] BETZ, G., WEHNER, G. K., TOTH, L., J. Appl. Phys. 45 (1974) 5312
- [12] HAAS, T. W., GRANT, J. T., DOOLEY III, G. J., J. Appl. Phys. 43 (1972) 1853.
- [13] FUJISAWA, N., SUGAWARA, T., TOI, K., MATOBA, T., KASAI, S., ITOH, S., Japan J. Appl. Phys. 13 (1974) 851.
- [14] FUNAHASHI, A., KASAI, S., MATOBA, T., FUJISAWA, N., JAERI-M5961 (1975) in Japanese.
- [15] HINNOV, E., J. Nucl. Mat. 53 (1974) 9.
- [16] EQUIPE TFR, Nucl. Fusion 15 (1975) 1053.
- [17] BEAVIS, L. C., J. Vac. Sci. Technol. 10 (1973) 386.
- [18] SUGIE, T., KASAI, S., SHIHO, M., private communication.
- [19] SATO, T., HIRAYAMA, T., MAENO, M., FUJISAWA, N., JAERI-M 6577 (1976) in Japanese.

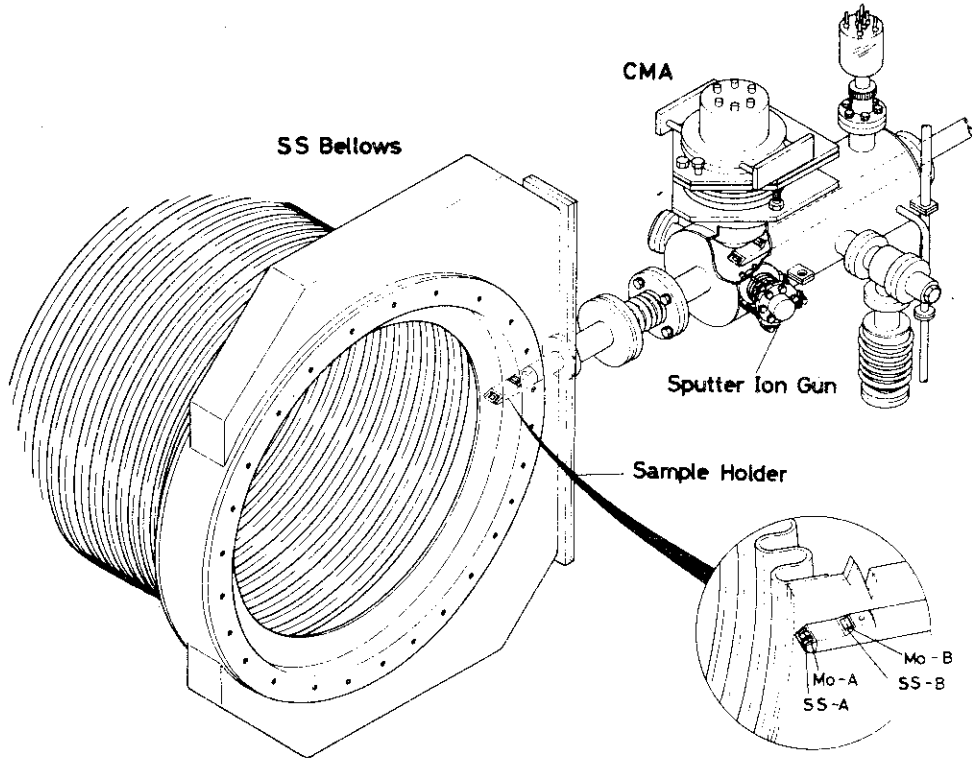


Fig. 1a Schematic view of the system for surface observation

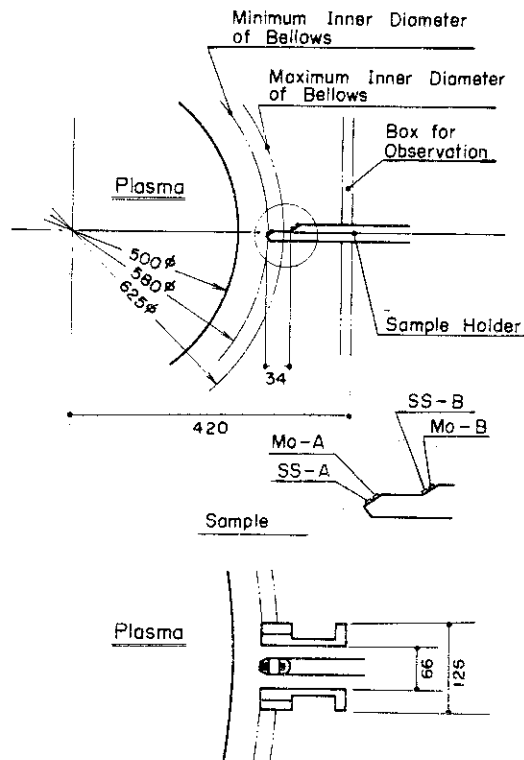


Fig. 1b Location of the samples exposed to the plasma

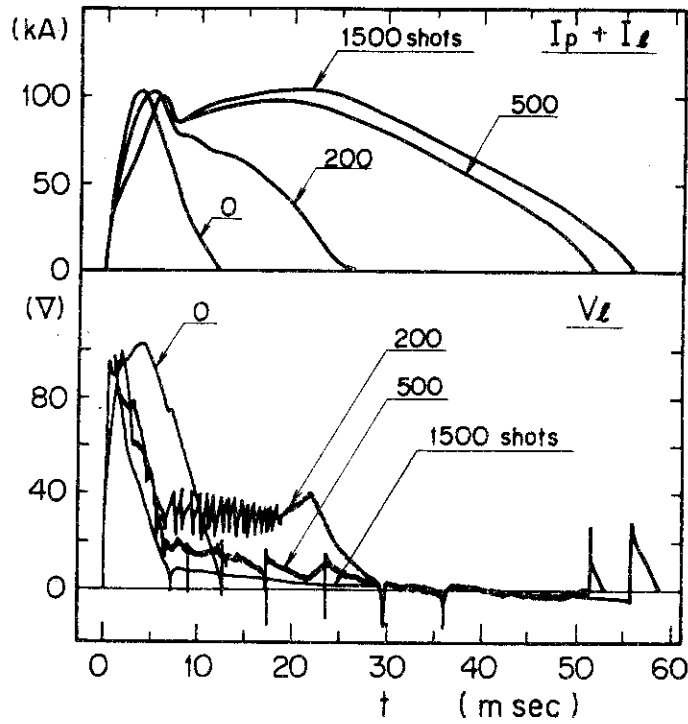


Fig. 2 The changes with cleaning pulses in the time behaviours of loop voltage V_l and total discharge current $I_p + I_l$ where I_p is the plasma current and I_l the liner one.

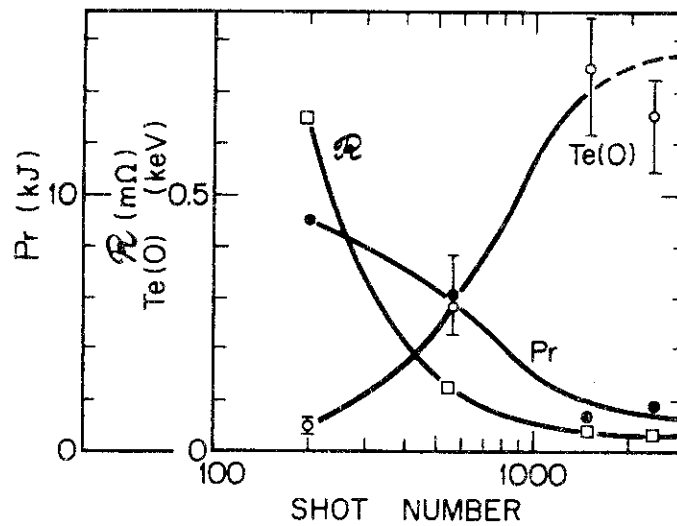


Fig. 3 The changes with cleaning pulses in the central electron temperature $T_e(0)$ and the plasma resistance at the peak of plasma current, and the radiation \mathcal{R} losses P_r integrated temporally during the discharge and spatially on the assumption that the distribution is homogeneous over the wall.

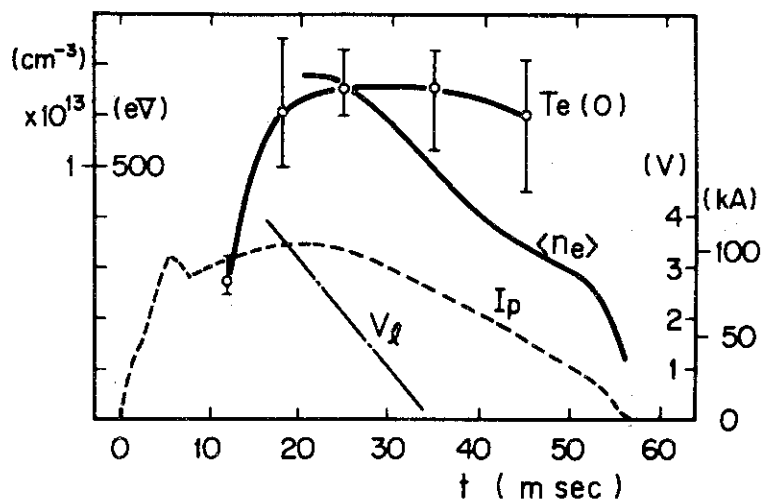


Fig. 4a The time behaviours of plasma current I_p , loop voltage V_l , mean line-of-sight density $\langle n_e \rangle$, and central electron temperature $T_e(0)$ after 2500 shots.

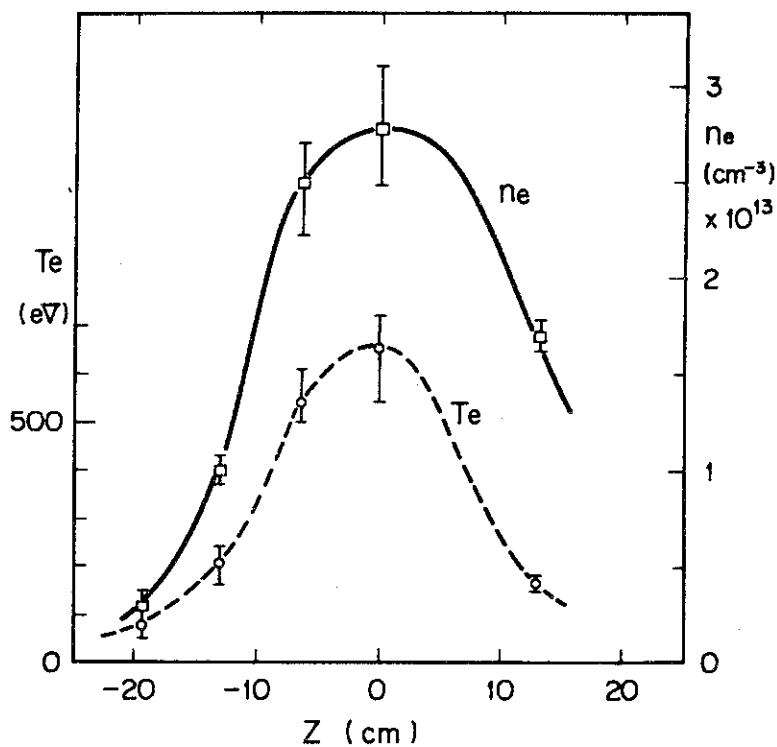


Fig. 4b The radial profiles of the electron temperature T_e and density n_e at the peak of plasma current after 2500 shots.

○ ● ○ ⊙ × * * △ △
 Mo Fe Cr Ni C O N Na Cl

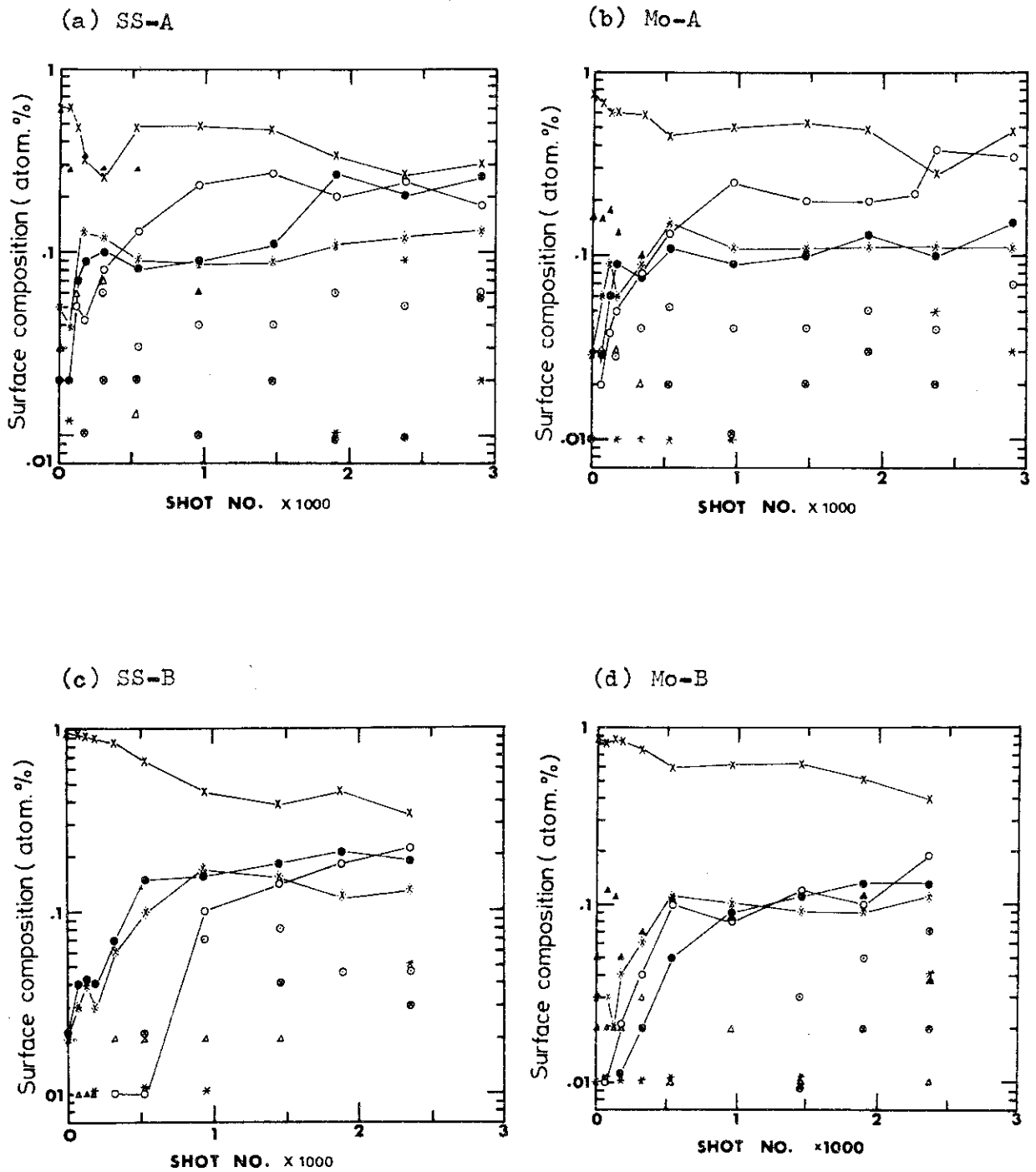


Fig. 5 The change of the surface composition with cleaning pulses except hydrogen and helium in the samples of (a) SS-A, (b) Mo-A, (c) SS-B and (d) Mo-B located as shown in Fig. 1b.

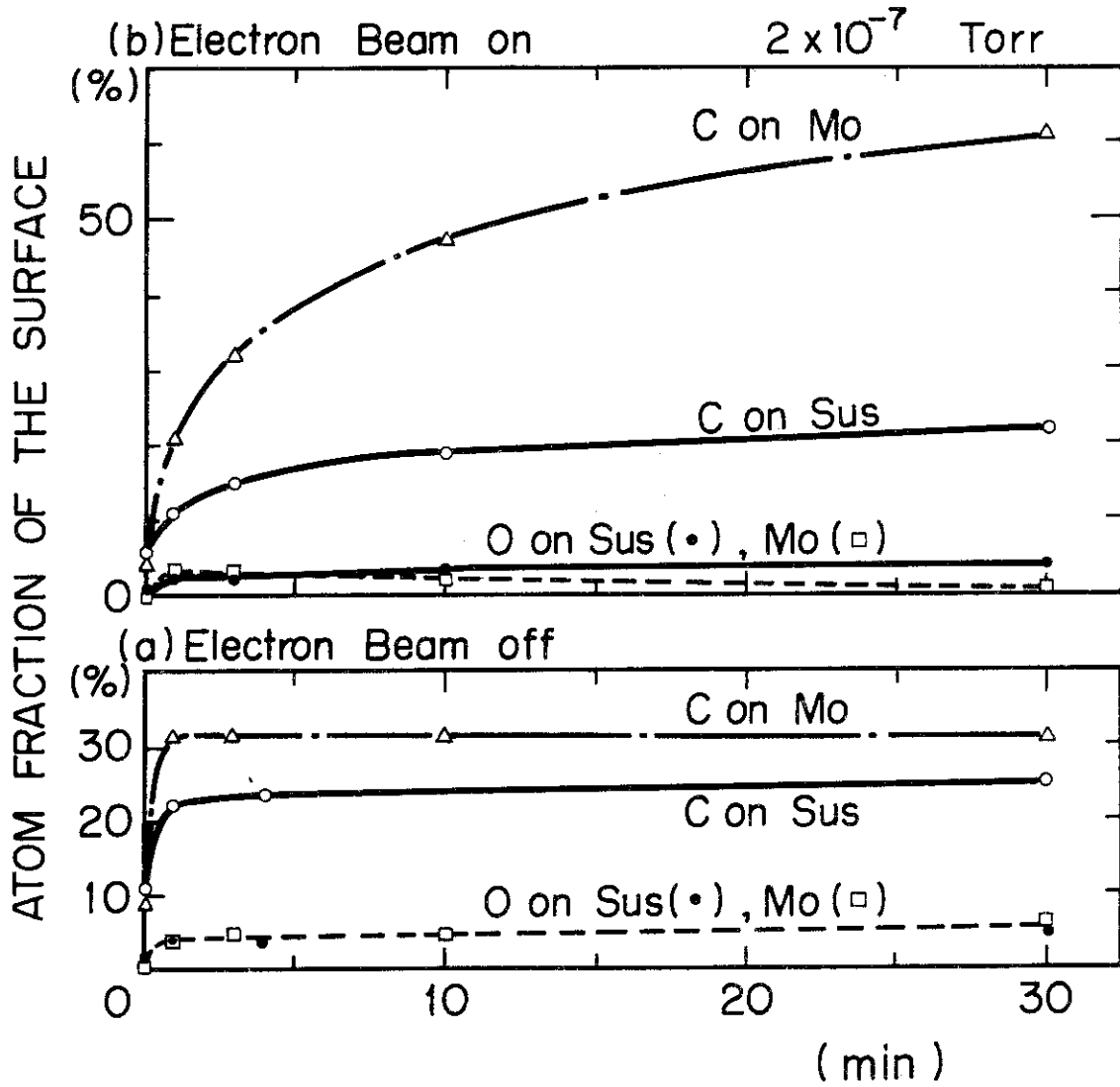


Fig. 6 The effect of (a) adsorption and (b) deposition of the ambient gas species on the surface under electron bombardment for AES.

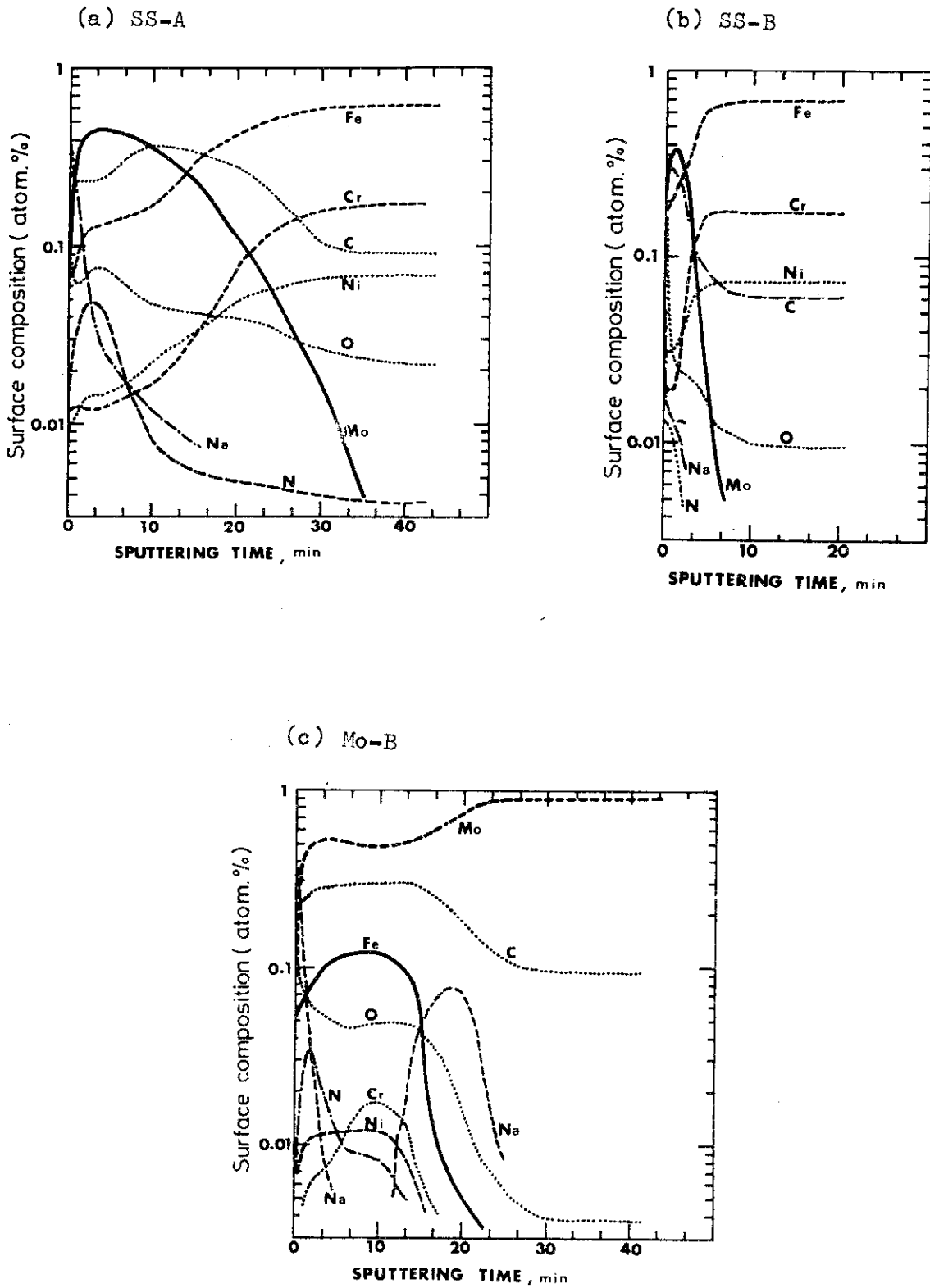


Fig. 7 The depth profiles of atomic composition in the samples of (a) SS-A, (b) SS-B and (c) Mo-B located as shown in Fig. 1b.

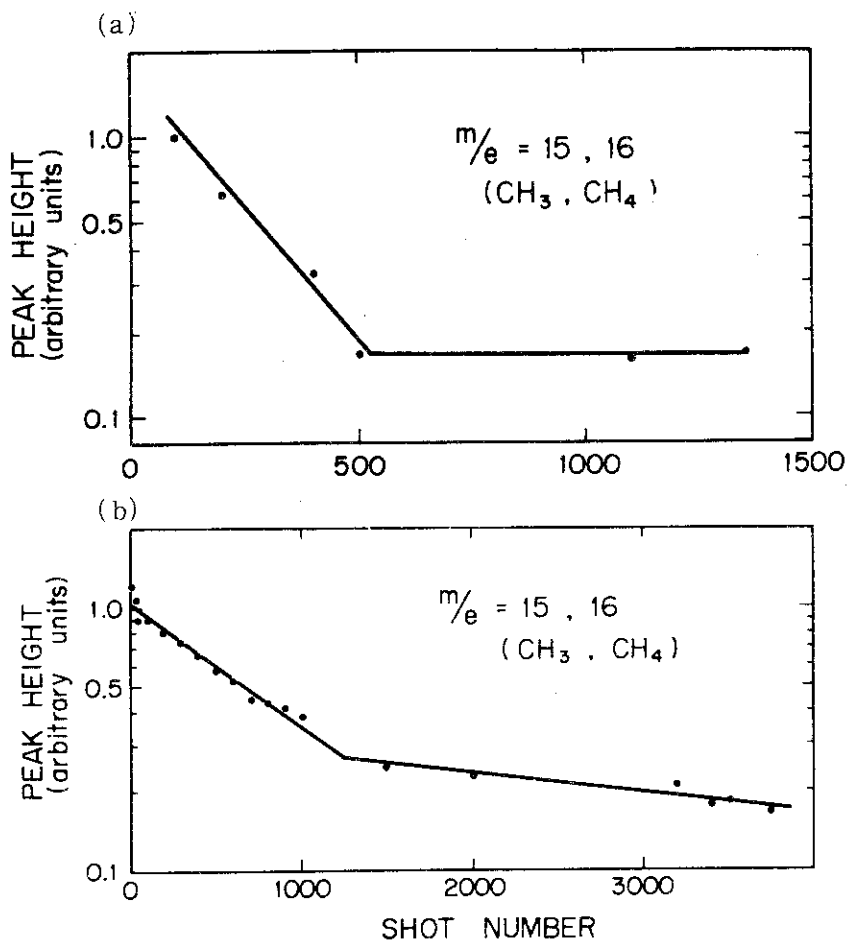


Fig. 8 The changes with cleaning pulses in the peak heights generated by the discharge in the mass peaks of $m/e = 15$ and 16 for (a) hydrogen and (b) helium discharge cleaning.

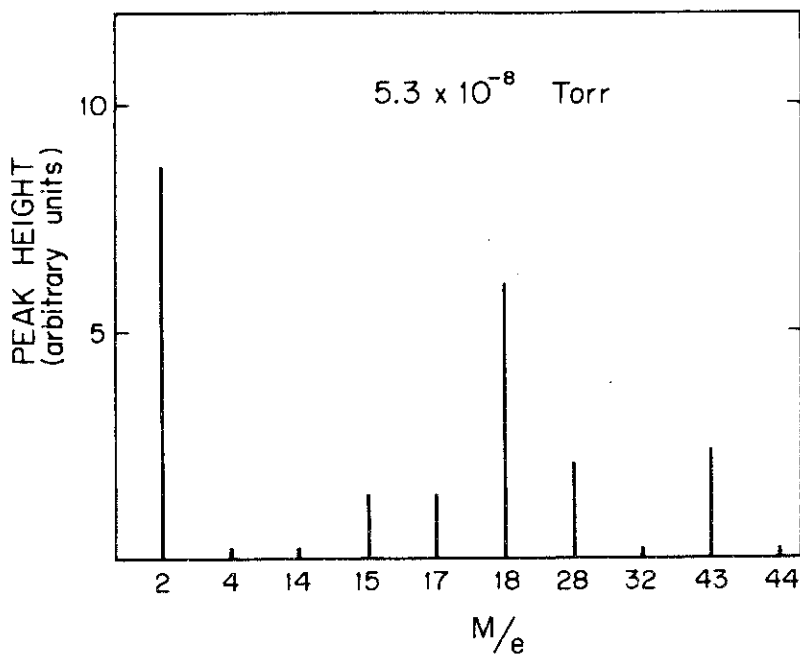


Fig. 9 Mass spectrum at the base pressure, 5×10^{-8} Torr.